INTERFACE

royalsocietypublishing.org/journal/rsif

Research

Cite this article: Wold ES, Lynch J, Gravish N, Sponberg S. 2023 Structural damping renders the hawkmoth exoskeleton mechanically insensitive to non-sinusoidal deformations. *J. R. Soc. Interface* **20**: 20230141. https://doi.org/10.1098/rsif.2023.0141

Received: 10 October 2022
Accepted: 25 April 2023

Subject Category:
Life Sciences–Physics interface

Subject Areas:
biomechanics, biomaterials

Keywords:
flight, exoskeleton, *Manduca*, structural damping

Author for correspondence:
Ethan S. Wold
e-mail: ewold3@gatech.edu

Downloaded from https://royalsocietypublishing.org/ on 22 May 2023

Structural damping renders the hawkmoth exoskeleton mechanically insensitive to non-sinusoidal deformations

Ethan S. Wold[1], James Lynch[3], Nick Gravish[3] and Simon Sponberg[1,2]

[1]School of Biological Sciences and [2]School of Physics, Georgia Institute of Technology, Atlanta, GA 30332, USA
[3]Mechanical and Aerospace Engineering, University of California San Diego, San Diego, CA 92161, USA

ESW, 0000-0002-9966-7715; SS, 0000-0003-4942-4894

Muscles act through elastic and dissipative elements to mediate movement, which can introduce dissipation and filtering which are important for energetics and control. The high power requirements of flapping flight can be reduced by an insect's exoskeleton, which acts as a spring with frequency-independent material properties under purely sinusoidal deformation. However, this purely sinusoidal dynamic regime does not encompass the asymmetric wing strokes of many insects or non-periodic deformations induced by external perturbations. As such, it remains unknown whether a frequency-independent model applies broadly and what implications it has for control. We used a vibration testing system to measure the mechanical properties of isolated *Manduca sexta* thoraces under symmetric, asymmetric and band-limited white noise deformations. The asymmetric and white noise conditions represent two types of generalized, multi-frequency deformations that may be encountered during steady-state and perturbed flight. Power savings and dissipation were indistinguishable between symmetric and asymmetric conditions, demonstrating that no additional energy is required to deform the thorax non-sinusoidally. Under white noise conditions, stiffness and damping were invariant with frequency, suggesting that the thorax has no frequency-dependent filtering properties. A simple flat frequency response function fits our measured frequency response. This work demonstrates the potential of materials with frequency-independent damping to simplify motor control by eliminating any velocity-dependent filtering that viscoelastic elements usually impose between muscle and wing.

1. Introduction

Muscles often act through series or parallel elastic elements to mediate movement, which have important consequences for locomotion. Locomotor springs such as tendons, ligaments, apodemes and exoskeleton serve many energetic roles, including absorbing, recycling and amplifying mechanical power [1–5]. In fulfilling these roles, elastic elements and their associated structures in an organism can act as a mechanical filter between muscle and output motion, as well as between external stimuli and sensory feedback systems [6–8]. The biomaterials that comprise musculoskeletal systems are often significantly dissipative, introducing energy losses and phase offsets between actuator force and appendage motion [4,9,10]. Nonideal transmissions such as latches and joints within locomotor systems can introduce additional energetic losses and contribute to local control of rapid movements by slowing the flow of quickly released elastic energy [11,12].

To account for this biomechanical filtering, an animal must tune the muscle force magnitude and timing it uses to produce a given movement or respond to a perturbation. During steady, sinusoidal and symmetric appendage movement, constant force and timing adjustments are largely unnecessary due to the single-frequency nature of these movements. However, steady locomotion often has asymmetric appendage movement [13–15]. Furthermore, during unsteady locomotion, musculoskeletal systems must contend with dynamic loading that

THE ROYAL SOCIETY PUBLISHING

© 2023 The Author(s) Published by the Royal Society. All rights reserved.

Downloaded from https://royalsocietypublishing.org/ on 22 May 2023

may contain a wide frequency band, impose transient perturbations, and often require rapid, adaptive control [16]. In these two common situations, body mechanics may exhibit strong frequency-dependent effects that differ from the body's response under single-frequency conditions, resulting in important locomotor consequences for the organism and necessitating concomitant, frequency-dependent tuning of the neuromuscular system.

The insect flight system presents a key example of how a highly complex elastic structure can affect energy flow during periodic movement. Many insects actuate their wings indirectly via deformations of the thoracic exoskeleton, which are created by the contraction of the flight power muscles [17]. Spring-like properties of the exoskeleton can reduce the power requirements for flapping flight via elastic energy exchange if inertial power requirements are significant [5,18,19]. Like all other biomaterials, the thorax also dissipates energy as it is deformed, contributing an irrecoverable power cost to flapping flight and introducing a phase difference between thorax stress and strain. Thus, the dynamics of the thorax present a filter on flight muscle force, impacting the transmission of energy from muscle to satisfy inertial and aerodynamic power costs and the timing of such energy flow to control the trajectory of the wing. While the thorax has been studied in an energetic context, the implications of thorax mechanics for control have been explored in far less detail [20–22].

Recent work has characterized the mechanical response of the hawkmoth *Manduca sexta* exoskeleton under purely sinusoidal deformations, showing that the exoskeleton is a linear spring with frequency-independent structural damping [19]. Dissipation due to structural damping from cycle to cycle depends on the amplitude of oscillation and not the frequency. This contrasts with viscous damping, which is a common model in biomaterials, especially muscle. During sinusoidal deformations, viscous materials dissipate energy per cycle proportional to both amplitude and frequency [23]. Structural damping is thought to originate from internal friction between fibrous or filamentous structures, making it similar to Coulomb sliding friction which also dissipates energy per cycle dependent on amplitude, but not velocity [24]. However, first-principles models of structural damping do not exist, and most successful modelling attempts rely on the use of a phenomenological characterization, or restrictions to single-frequency motion [25].

While structural damping is present at the whole thorax level, this property has also been demonstrated in resilin, the constituent elastic protein that gives insect joints much of their resilience, as well as the whole joints of cockroaches during out-of-plane rotation [26,27]. Recent modelling work has shown that structural damping is a key determinant of the dynamic efficiency of flapping insects [28]. Altogether, while the presence of structural damping has been demonstrated in multiple insects, its relevance beyond steady, periodic conditions and impacts on motor control have not been explored. It is possible that frequency-dependent behaviour emerges in non-sinusoidal regimes, consisting of more than one deformation tone. A common form of frequency-dependent material behaviour found in biology is linear viscous damping; however, given that previous work has found this model to be a poor fit for the hawkmoth thorax, it is more likely that any emergent frequency dependence arises from other factors such as nonlinearities in the thoracic shell, the friction-like underpinning of structural damping phenomenon or by higher-order thoracic vibration modes [19]. If the insect thorax exhibits frequency dependence under non-sinusoidal deformation, within-wingstroke frequency modulation would require frequency-dependent tuning of muscle timing to compensate for phase lags. If a structural damping model holds in non-sinusoidal regimes, frequency modulation could be achieved with the same muscle force magnitude and phasing as in single-frequency wingstrokes.

Non-sinusoidal characteristics are well-documented in the stroke-angle kinematics of multiple insects (figure 1*a*), though it is reasonable to ask whether such non-sinusoidality is manifested in the thorax itself during realistic behaviour. Indeed, Ando *et al*. [20] make the only direct measurements of thorax deformations in *Manduca* and demonstrate clear asymmetric behaviour in thorax displacements [20]. Combined with the evidence suggesting that the hawkmoth wing hinge is well-approximated as linear, has low series elastic compliance, and is at least partially back-drivable, it is very likely that some degree of asymmetry at the level of the thorax is necessary to generate substantial asymmetry in wing-tip kinematics [32–34]. Likewise, external perturbations to the wing are likely to be transmitted through the wing hinge as non-periodic, transient thorax deformations. There is certainly great subtlety in the mechanism by which asymmetries at the thorax level result in modification of all three Euler angles, not just stroke plane angle. In the light of the fact that we lack detailed knowledge regarding the link between precise thorax deformations and three-dimensional wing kinematics, we focus our attention on two classes of non-sinusoidal deformation likely experienced by moths in flight, shedding light on a general frequency independence in the thorax and its implications for flight control.

We subjected *Manduca* thoraces to two different types of mechanical stimuli: asymmetric, periodic movements and band-limited white noise. We generated asymmetric displacement signals that create asymmetry between upstroke and downstroke, mimicking wing-tip asymmetries observed in free flight [29] and thorax deformations in tethered flight [20]. Such asymmetries include harmonics of the fundamental that may excite frequency-dependent thorax behaviour. Then, we subjected the thorax to band-limited white noise to determine its response to displacement signals with substantial power over a wide frequency band. This condition simulates potential deformations that a hawkmoth may experience while manoeuvring to remain stable in the air in response to aerodynamic perturbations, turbulence or changing wind speeds [29,35,36]. Similar wingstroke irregularities also may be introduced or exacerbated when the wings become damaged [37–39]. We predict that the storage and dissipative characteristics of the thoracic spring will be the same for a given deformation amplitude, regardless of asymmetry or the frequency content of the deformation.

2. Material and methods

2.1. Animals

Manduca sexta were obtained as pupae from colonies based at the University of Washington and Case Western Reserve University. Moths were stored in a humidity and temperature controlled incubator on a 12 L:12 D cycle. All animals were used within seven days of eclosion, and moth mass was equal to 2.24 ± 0.49 g. Both male and female moths were used.

Downloaded from https://royalsocietypublishing.org/ on 22 May 2023

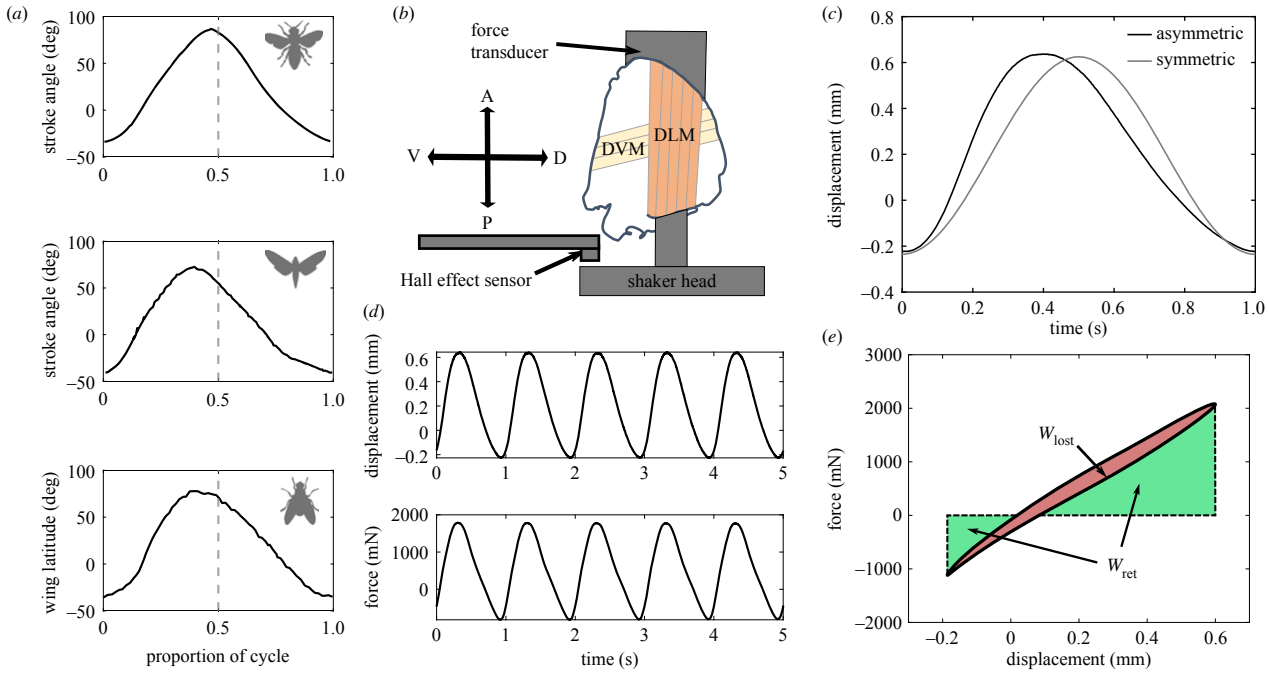

Figure 1. (*a*) Kinematic data from bumblebee (top), hawkmoth (middle), and fly (bottom) flight showing various degrees of non-sinusoidality and asymmetry [15,29,30]. (*b*) Schematic of hawkmoth thorax mounted to the head of an electrodynamic shaker and a force transducer [19,31]. The dorsolongitudinal (DLM, downstroke) and dorsoventral (DVM, upstroke) muscles are labelled and act through the thoracic shell to produce wingstrokes. A Hall effect sensor measures displacement from a magnet embedded in the shaker head. (*c*) Example input signals for the symmetric and asymmetric deformations at 1 Hz. The asymmetric signal shows a clear difference in the rise and fall time of the oscillation. (*d*) Representative timeseries for an asymmetric experiment at 1 Hz showing that asymmetries in the displacement waveform are recapitulated in the force waveform. (*e*) Representative force–displacement plot with dissipated and returned work highlighted in red and green respectively. The plot is not symmetric about the origin because the thorax has been pre-compressed.

2.2. Thorax preparation

Our preparation was based on that of Gau *et al*. [19]. Moths were anaesthetized in a refrigerator for approximately 20 min, and the thorax was immediately isolated from the head and abdomen. The scales, wings, legs and first thoracic segment were removed to isolate the second and third thoracic segments, which are the regions responsible for indirect actuation of the wings. The thoracic ganglion was carefully severed, accessed via the opening created by removing the head, to eliminate residual nervous system activity. Special care was taken to sever the flight muscle so that any spontaneous activity would not transmit appreciable force to the exoskeleton. Previous work has demonstrated that passive musculature contributes negligibly to thorax elasticity and damping, so severing these muscles likely did not meaningfully affect our measured thorax forces [19].

2.3. Shaker mounting and preparation

We again follow the methods of Gau *et al*. [19] with minor adjustments. Custom three-dimensional printed mounts were secured to the posterior phragma and the scutum with cyanoacrylate glue. Glue was applied in a thin layer only on the regions of the thorax directly in contact with the mounts, resulting in a rigid connection on each end. Importantly, these attachment regions do not deform substantially during flight and are not responsible for elastic energy storage; therefore we were not concerned with the small amount of glue modifying our measured thorax behaviour [19]. The scutum mount was screwed into a 10 N force transducer with a resonant frequency of 300 Hz (FORT1000, World Precision Instruments, Sarasota, FL), and the posterior phragma mount was rigidly attached to the shaker head. The force transducer was attached to a micromanipulator, giving us precise control over the thorax's rest length. Importantly, we aligned the thorax such that deformations occurred along the axis that the downstroke muscle would contract in the live animal (figure 1*b*). We measured the weight of the posterior mount and glue before securing it to the thorax and returned the system to this weight after mounting the thorax to the shaker. We then pre-compressed the thorax by 0.21 mm using the micromanipulator to match the average measured *in vivo* operating length of the DLM during tethered flight [40]. An analogue Hall effect sensor (DRV5053-Q1, Texas Instruments, Dallas, TX) was used to measure displacement from a permanent magnet embedded in the shaker head. The Hall effect sensor was calibrated daily using a fifth order polynomial immediately prior to mounting the first specimen. The shaker head itself was driven by an electrodynamic vibration testing system (VTS600, Vibration Testing Systems, Aurora, OH) [31]. Data for all experiments were collected at 10 kHz.

2.4. Deformations

We first prescribed sinusoidal deformations at both 1 and 25 Hz and a physiological peak-to-peak displacement of 0.92 mm, equivalent to 4.5% strain amplitude of a typical 10 mm long thorax. The 25 Hz condition matches *Manduca*'s real wing beat frequency [29]. While there is likely some small variation in strain amplitudes between individuals, the protocol of using a mean strain across all individuals has been established in the literature [40,41]. From our length measurements, we calculated that the amplitude of our deformations corresponds to $4.5 \pm 0.15\%$ thorax length across all individuals. We then prescribed an asymmetric sinusoid generated by splicing together two sine waves to create an upstroke and downstroke of different frequencies (figure 1*b*,*c*). The intrinsic nonlinear dynamics of our shaker filtered these signals, smoothing out the connections between each sinusoid, but preserved substantial asymmetry which was sufficient to test our hypotheses. Throughout we report the resulting strains rather than the prescribed ones.

We tested asymmetry at an average frequency of 1 Hz, so that we could reliably generate the same asymmetry (61% of a cycle spent on extension phase) from trial to trial. We also performed asymmetric trials at 25 Hz to confirm that the thorax's general response to non-sinusoidality persists at wing beat frequency. At this higher frequency, the shaker's large inertia introduced

Downloaded from https://royalsocietypublishing.org/ on 22 May 2023

filtering dynamics that made it extremely difficult to produce large, repeatable asymmetries, requiring many more trials to obtain viable data. In five individuals, we were able to generate 25 Hz asymmetries which had a different shape from the 1 Hz asymmetries but preserved strong non-sinusoidality and a reliable asymmetry (0.55% of a cycle spent on extension phase). When compared statistically with a *t*-test to the fraction of a cycle spent on extension phase in symmetric oscillations, a significant difference was found with $p \ll 0.001$ at both 1 and 25 Hz. The average frequency was defined as the inverse of the duration of one asymmetric upstroke and downstroke.

Finally, we prescribed band-limited white noise for 5 s, with an upper frequency limit of 25 Hz. The shaker also filtered these signals, but the resulting deformations had substantial power density across the 25 Hz band. At frequencies above 25 Hz, we found it difficult to generate reliable asymmetries and white noise with our shaker at our desired amplitudes, so we chose the *in vivo* wing beat frequency as our upper frequency limit.

2.5. Data analysis

We calculated components of mass-specific mechanical power by integrating the force–displacement curves, multiplying the resulting energies by the frequency of oscillation, and dividing by body mass [19] (figure 1*e*). We define P_{return} to be the mechanical power savings from elastic energy storage and P_{lost} to be the oscillation-averaged dissipated power. P_{in} is the total mechanical power required to deform the thorax and is the sum of P_{return} and P_{lost}. For asymmetric conditions, we used the average frequency as defined above, either 1 or 25 Hz. While this does represent an approximation since asymmetric oscillations do not have a single frequency, any frequency-dependent behaviour will be evident in the energy computation from the force–displacement loop. Furthermore, this choice allows us to make like-to-like comparisons of power between the symmetry conditions at the same average frequency, and compare mass-specific powers to existing literature values.

We use the structurally damped spring–damper material model previously established for cockroach leg joints and hawkmoth thorax to compute thorax material properties [19,27]. This model consists of a spring with stiffness k in parallel with a damper that is characterized by a structural damping parameter γ. There are two common mathematical formulations: one utilizes a complex spring stiffness (equation of motion $f(t) = k(1 + \gamma j)x(t)$), while the other treats the damper as an equivalent viscous damper with a frequency-dependent coefficient (equation of motion $f(t) = kx(t) + (k\gamma/\omega)\dot{x}(t)$) [25,28]. These two models both result in frequency independence and are equivalent for deformations of a single frequency, as we show below.

To calculate a spring stiffness and structural damping parameter, we applied a fast Fourier transform (FFT) to our force and displacement time series. We divided the transformed force in the frequency domain by the transformed displacement to calculate the complex modulus. The complex modulus is a frequency-dependent quantity, whose real part represents the elastic characteristics of a material, and whose imaginary part represents the dissipative characteristics. The effective stiffness (k) of the thorax was calculated from the real part of the complex modulus and the structural damping parameter γ was calculated from the complex part, as shown in the following equations:

$$k(\omega) = E'(\omega)\frac{A}{L} \tag{2.1}$$

and

$$\gamma(\omega) = \frac{E''(\omega)}{E'(\omega)}. \tag{2.2}$$

Here, $E'(\omega)$ is the real part of the complex modulus, $E''(\omega)$ is the imaginary part of the complex modulus, A is the area of muscle attachment, and L is thorax length. Since our experiments were carried out at either 1 Hz or 25 Hz, we extracted the material properties at these two frequencies. This method is appropriate for symmetric and asymmetric force–displacement loops that are well fit by an ellipse, as defined by the complex modulus. The average r^2 of such elliptic fits for asymmetries at 1 Hz and 25 Hz were 0.88 and 0.83, which affirm that evaluating the complex modulus at the fundamental should result in accurate parameter estimates.

For the white noise data, we applied a time-averaged FFT to force and displacement with an overlapping Hanning window. After windowing, the frequency resolution of our spectra was 0.6 Hz. Like the asymmetry data, we compute a complex modulus by dividing the force and displacement in the frequency domain. Since the white noise stimulus contained frequencies up to 25 Hz, the complex modulus can be thought of as the frequency response of the thorax over this band. Using Newton's second law for the vibrating thorax, we derived an analytical prediction for the frequency response function (FRF) of a structurally damped spring with negligible inertia:

$$f(t) = kx(t) + \frac{k\gamma}{\omega}\dot{x}(t), \tag{2.3}$$

where x is the linear displacement of the thorax, k is the linear thorax stiffness, γ is the damping parameter, and $f(t)$ is the force produced by deforming the thorax. We neglect inertia of the wings, since the wings are not attached in our preparation, and the very small deformed mass of muscle and cuticle does not affect thorax material response [19]. Likewise, we neglect shaker mass as we analyze only displacements and forces measured at the level of the thorax. We utilize the equivalent viscous damper formulation of a structural damper, which manifests in frequency-independent damping for sinusoidal motion. The velocity of a single-frequency sinusoidal trajectory ($\dot{x}$) will be linearly proportional to the frequency of oscillation. This factor of frequency cancels out with the $1/\omega$ in the damping coefficient to yield a frequency-independent FRF. Taking the Laplace transform of both sides and solving for the frequency response function yields

$$T(j\omega) = \frac{X(j\omega)}{F(j\omega)} = \frac{1}{k + (k\gamma/\omega)(j\omega)} = \frac{1}{k(1 + \gamma j)}. \tag{2.4}$$

This FRF has a magnitude and phase given by the following:

$$|T(j\omega)| = \frac{1}{\sqrt{k^2(1 + \gamma^2)}} \tag{2.5}$$

and

$$\angle T(j\omega) = \tan^{-1}\gamma. \tag{2.6}$$

Note that the frequency variable ω disappears from the magnitude and phase of the FRF, reflective of the frequency-independent property of a structural damper. In the regime of $\gamma \ll 1$, as is likely the case in *Manduca*, these expressions predict a constant gain and phase of $1/k$ and γ respectively [19]. We used unpaired, two-sample *t*-tests with a significance threshold of 0.05 to compare each quantity of interest (thoracic powers, stiffness, damping coefficient) between symmetric and asymmetric conditions. All data are reported as mean ± one standard deviation.

3. Results

3.1. Symmetric and asymmetric deformations do not affect thorax material properties

Under symmetric deformation at 1 and 25 Hz (figure 2*a*,*b*) as well as asymmetric deformation at 1 Hz (figure 2*c*), thoraces

Downloaded from https://royalsocietypublishing.org/ on 22 May 2023

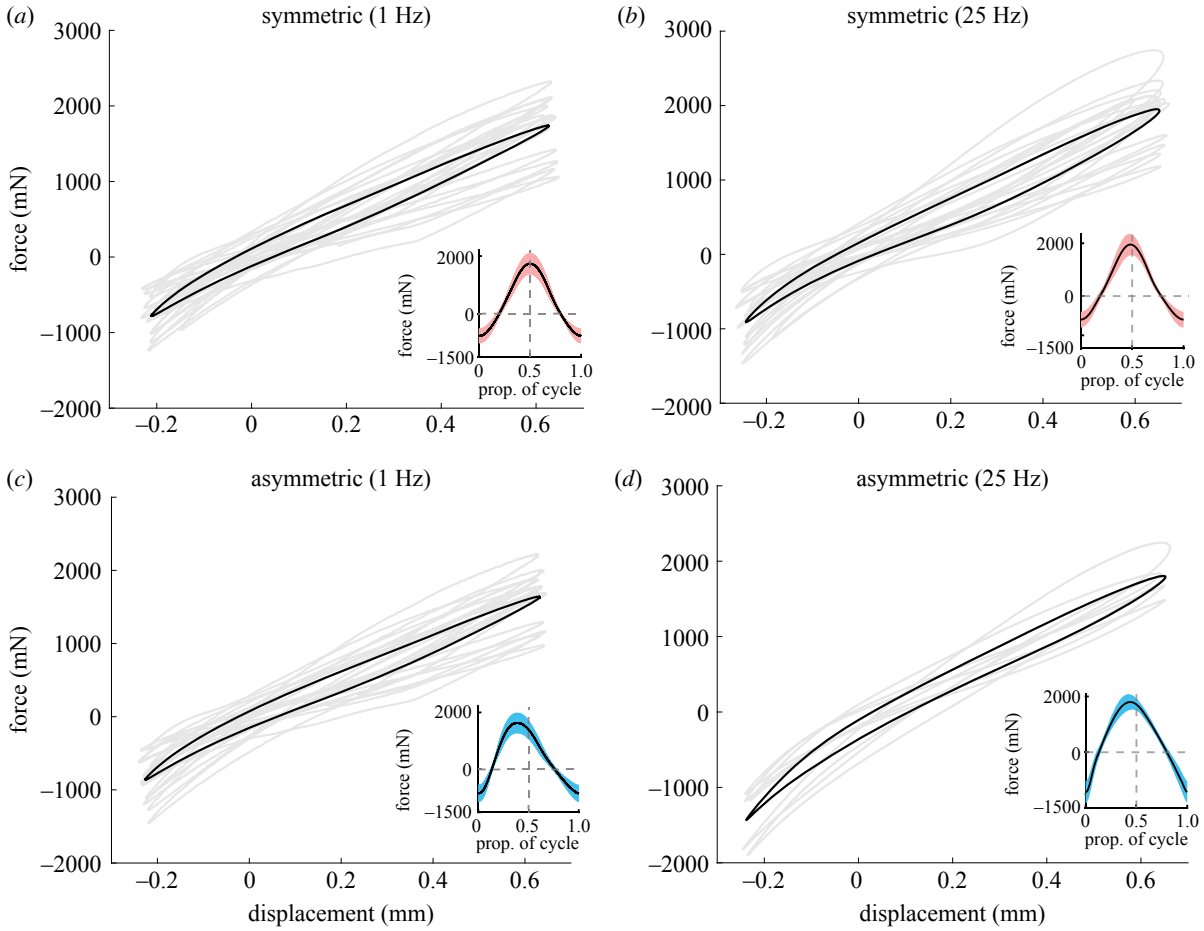

Figure 2. Force–displacement data across all experimental conditions. Mean force–displacement loops (black line) for all individuals under symmetric displacements at (*a*) 1 Hz ($N = 14$) and (*b*) 25 Hz ($N = 14$), and asymmetric displacements at (*c*) 1 Hz ($N = 14$) and (*d*) 25 Hz ($N = 5$). Displacements across all conditions were 0.92 mm peak-to-peak. Oscillations at 25 Hz averaged slightly larger forces than oscillations at 1 Hz. Light grey lines show individual variation. Insets show mean ± standard deviation forces for a single oscillation.

exhibit characteristics of a weakly damped, linear spring as evidenced by the relatively constant slope of each loop. In the asymmetric 25 Hz case (figure 2*d*), there appears to be a slight downward curvature of the loop in tension compared to the symmetric case. Our sign convention is such that positive displacements represent compression while negative displacements represent tension.

To quantitatively compare the shapes of the symmetric and asymmetric force–displacement loops, we compute stiffness and the structural damping factor under each symmetry and frequency condition. We found no statistically significant differences between stiffness or damping at either 1 Hz (table 1, figure 3*a*) or 25 Hz (table 1, figure 3*b*), as determined by unpaired two-sample *t*-tests. The slight stiffening (10%) we observed in the 25 Hz asymmetric case compared to the symmetric case (figure 3*b*) may be the result of the nonlinear properties of the exoskeleton being excited by a higher frequency asymmetry, therefore resulting in the slight downward curvature of the force–displacement loop (figure 2*d*) and increased peak force during tension. All stiffness values are somewhat higher than the stiffness found by Gau *et al.*, but result in peak forces within the range of the previously reported force-producing capacity for the *Manduca sexta* DLM [41]. We do not explicitly consider active muscle stiffness, since *Manduca* flight muscle stiffness is relatively low compared to the thorax and likely does not contribute significantly to total flight power costs [19,34,41].

3.2. Peak and cycle-averaged mechanical power is equivalent during symmetric and asymmetric deformations

To determine whether deviations from a sinusoidal trajectory modify thoracic energetics, we compared peak power, power returned and power lost during each symmetry and frequency condition. Peak power and peak load were statistically indistinguishable between symmetric and asymmetric conditions at both 1 Hz and 25 Hz (table 1, figure 3*c*,*d*). Likewise, returned and lost power were indistinguishable between symmetric and asymmetric conditions at both 1 Hz and 25 Hz, which is consistent with our prediction that structural damping losses should only depend on deformation amplitude (table 1, figure 3*e*,*f*). The slight stiffening observed in figure 3*b* does not significantly affect power saved by the thoracic spring; therefore we suggest that it is not biologically relevant, at least under the conditions studied here.

3.3. The thorax has a flat frequency response curve

To assess whether a signal with a continuously changing frequency content modifies exoskeleton energetics, we subjected the thorax to band-limited white noise deformation signals (figure 4*a*). Filtering of our white noise signals by the shaker results in a spectrum that is not perfectly uniform over the band of interest, but still shows a clear cutoff

Downloaded from https://royalsocietypublishing.org/ on 22 May 2023

Table 1. All measurements reported for each frequency and symmetry conditions. Data are reported as mean ± one standard deviation. *p*-values reported for *t*-test comparisons of measurements taken at the same frequency but with different symmetry conditions.

condition	frequency	quantity	value	*p*-value
symmetric	1 Hz	k	2.93 ± 0.73 kN m^{-1}	0.66
asymmetric	1 Hz	k	3.05 ± 0.73 kN m^{-1}	
symmetric	1 Hz	γ	0.113 ± 0.027	0.67
asymmetric	1 Hz	γ	0.118 ± 0.034	
symmetric	25 Hz	k	2.78 ± 0.69 kN m^{-1}	0.14
asymmetric	25 Hz	k	3.33 ± 0.68 kN m^{-1}	
symmetric	25 Hz	γ	0.095 ± 0.035	0.71
asymmetric	25 Hz	γ	0.101 ± 0.022	
symmetric	1 Hz	P_{peak}	1.06 ± 0.34 W kg^{-1}	0.26
asymmetric	1 Hz	P_{peak}	1.22 ± 0.39 W kg^{-1}	
symmetric	1 Hz	F_{peak}	1.66 ± 0.40 kN	0.28
asymmetric	1 Hz	F_{peak}	1.83 ± 0.40 kN	
symmetric	25 Hz	P_{peak}	31.83 ± 10.83 W kg^{-1}	0.06
asymmetric	25 Hz	P_{peak}	21.41 ± 7.04 W kg^{-1}	
symmetric	25 Hz	F_{peak}	1.65 ± 0.41 kN	0.15
asymmetric	25 Hz	F_{peak}	1.96 ± 0.35 kN	
symmetric	1 Hz	P_{return}	0.248 ± 0.082 W kg^{-1}	0.69
asymmetric	1 Hz	P_{return}	0.235 ± 0.082 W kg^{-1}	
symmetric	1 Hz	P_{lost}	0.084 ± 0.025 W kg^{-1}	0.20
asymmetric	1 Hz	P_{lost}	0.082 ± 0.023 W kg^{-1}	
symmetric	25 Hz	P_{return}	7.06 ± 2.25 W kg^{-1}	0.75
asymmetric	25 Hz	P_{return}	6.69 ± 2.05 W kg^{-1}	
symmetric	25 Hz	P_{lost}	2.90 ± 1.29 W kg^{-1}	0.38
asymmetric	25 Hz	P_{lost}	2.32 ± 0.94 W kg^{-1}	

frequency at 25 Hz (figure 4*b*). Signal power present at higher frequencies is quite low, resulting in an erratic frequency response, so we plot only up to 25 Hz. Regardless, our conclusions do not depend on the stimulus being perfectly white, since we are interested in testing the thorax's response to a generalized irregular deformation.

We measured the frequency response function in the thorax to have a gain and phase that are relatively flat with frequency (figure 4). We found an average gain and phase of 3.3 kN m^{-1} and 0.18 rad at 25 Hz, respectively. These values are in accordance with published stiffness and damping factors from hawkmoths and cockroaches [19,27]. They are towards the higher end of the estimates of stiffness and damping from oscillatory deformation in this paper. Our theoretical prediction for a structurally damped spring with negligible inertia fits well on top of our measured data. Fitting a linear viscous damping model would require the selection of a constant viscous damping coefficient, which decreases sharply with frequency in the *Manduca* thorax [19]. As such, the viscous model is likely a poor representation of thorax mechanics and we do not consider it further. Since our definitions of gain and phase correspond directly to stiffness and structural damping coefficient, these results are equivalent to stating that there is no substantial increase in stiffness or damping during irregular motion containing frequencies in the band we tested. However, data on symmetric oscillations of *Manduca* thoraces at frequencies up to 90 Hz lead us to believe that this trend likely extends significantly beyond the 25 Hz limit imposed by our technological constraints [19].

4. Discussion

4.1. The thorax is mechanically insensitive to asymmetric oscillations

Our results demonstrate that there does not exist a significant additional energetic cost to deform the thorax asymmetrically. If velocity-dependent behaviour were a dominant source of dissipation in the thorax, we would expect a distortion of the asymmetric force–displacement loop relative to the symmetric one that would manifest in a measurably greater lost power, since its frequency changes within a single period of oscillation. By contrast, we observe the same lost power as observed during symmetric deformations, as demonstrated by the same hysteretic loops (figure 2*b*,*d*). Frequency-independent dissipation can be understood in the context of the single-tone model of structural damping. The dissipated energy per cycle can be computed as the integral of the damping force $(k\gamma/\omega)\dot{x}$, yielding $\pi k\gamma X_o^2$, where X_o is the deformation amplitude. The average power dissipated per cycle will be this energy

Downloaded from https://royalsocietypublishing.org/ on 22 May 2023

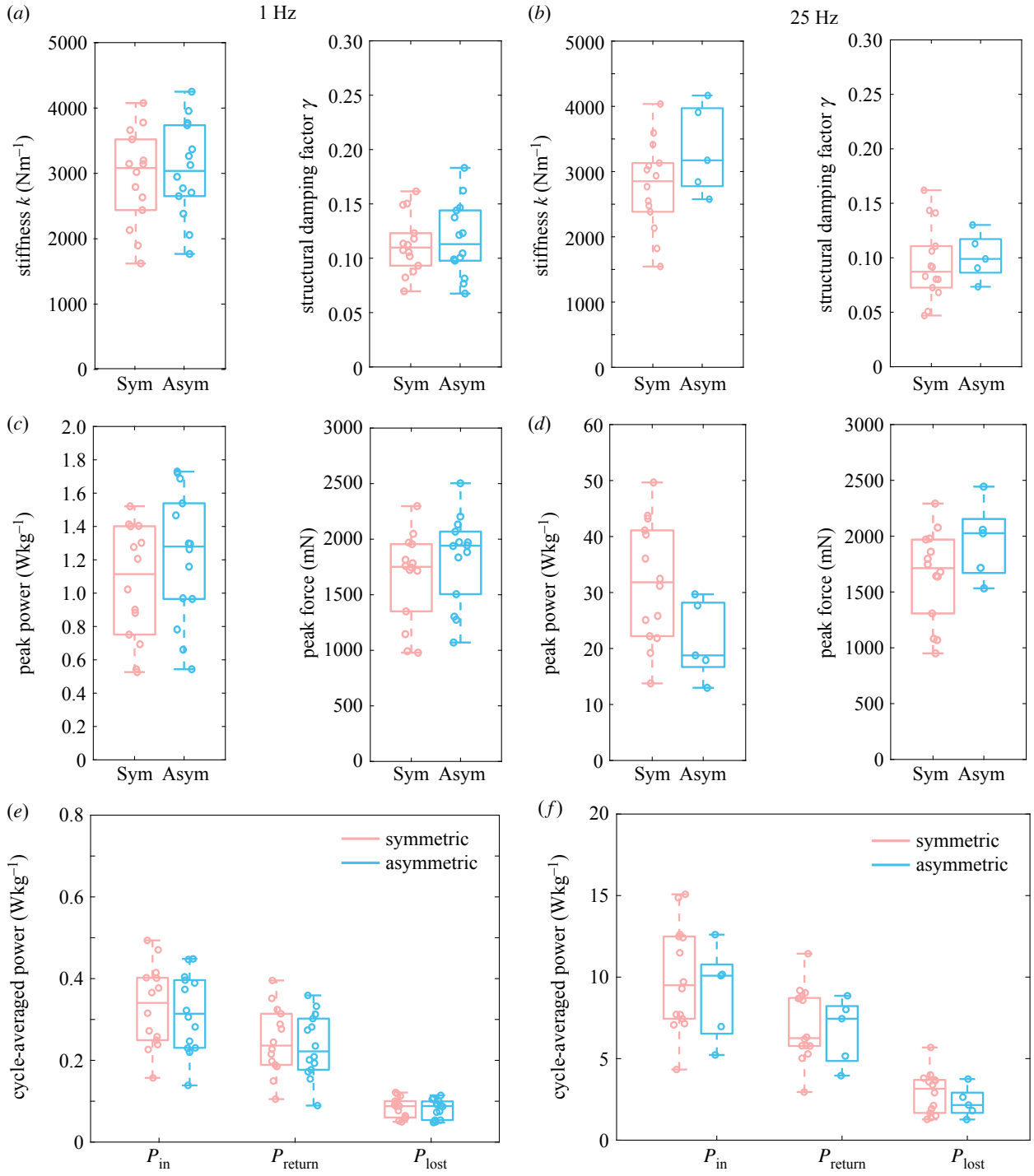

Figure 3. Material properties and thoracic powers for symmetric and asymmetric deformations. Stiffness and the structural damping constant do not differ between oscillation conditions at 1 Hz (*a*) and 25 Hz (*b*) regardless of whether the deformation is symmetric or asymmetric. Mass-specific peak power and peak load do not differ between oscillation conditions at 1 Hz (*c*) and 25 Hz (*d*) regardless of asymmetry. Mass-specific total power expended, dissipated and returned do not differ between symmetric and asymmetric conditions at either 1 Hz (e) or 25 Hz (*f*).

multiplied by the average oscillation frequency. Even though asymmetries are not single-tone, our empirical data demonstrate that the frequency-independent dissipation that this analysis predicts is indeed general. For example, applying the equation above for an average frequency of 25 Hz yields a predicted lost power of 1.96 W kg^{-1} in the symmetric case, and 2.5 W kg^{-1} in the asymmetric case, which are comparable to our measurements of lost power from integrating force–displacement loops, reported in table 1.

This energetic insensitivity to asymmetry persists at both physiologically relevant wingbeat frequencies for *Manduca* (25 Hz) and for frequencies an order of magnitude lower (1 Hz). One implication of these results is that observations of thorax mechanics at frequencies far below 25 Hz are likely representative of mechanics at 25 Hz. Measurements of insect thorax mechanics that can be made more easily at a low frequency may then be scaled up by frequency to draw conclusions about higher frequencies. While we did not explicitly test asymmetry at frequencies much higher than 25 Hz due to technical constraints, purely sinusoidal experiments have demonstrated frequency independence up to at least 90 Hz in *Manduca* [19]. Therefore, it is very likely that asymmetries are energetically inconsequential at higher frequencies as well. Note that under a viscous damping model, dissipated energy per cycle is equal

Downloaded from https://royalsocietypublishing.org/ on 22 May 2023

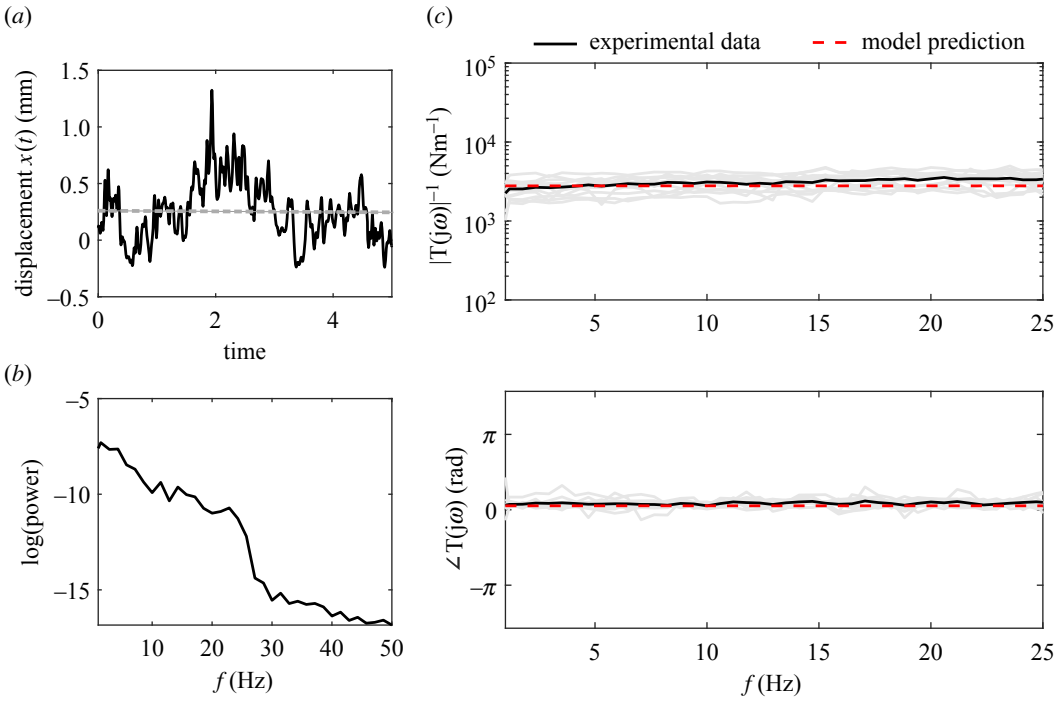

Figure 4. Frequency response of the thorax and characterization of damping. (*a*) A representative white noise displacement time series mimics an irregular perturbation with large frequency content. Note that the mean displacement shown by the grey dashed line is around 0.21 mm, corresponding to the prescribed thorax precompression. (*b*) The mean power spectrum of the detrended measured displacements in all individuals shows the majority of power within the 1–25 Hz band. (*c*) Gain and phase, which are analogous to stiffness and the damping constant, are flat with frequency, which is in accordance with the prediction from an analytical structurally damped frequency response function. Black lines show the mean and light grey lines show individual variation ($N = 12$).

to $\pi c \omega X_o^2$. If we assume a simplified asymmetry with upstroke frequency and downstroke frequencies matching our prescribed asymmetry, the viscous model predicts a modest 5–10% increase in lost power compared to the structurally damped case. This is not unexpected, since the symmetric and asymmetric inputs have the same average period, and so the difference between upstroke and downstroke frequency will not be enormous. However, our comparisons of the 1 Hz and 25 Hz conditions affirm that a structurally damped model is indeed appropriate in the asymmetric regime, regardless of the origin of frequency-dependent behaviour.

Structural losses themselves comprise a relatively small component of an insect's total energy budget, when compared to aerodynamic and inertial costs [19] but are not negligible. Indeed, when comparing their magnitude to recent estimates of aerodynamic power requirements for *Manduca*, structural losses account for up to 20% of all dissipative power costs for the animal, a proportion that could aid in wing deceleration at the expense of overall efficiency [19]. Extending this argument, recent numerical and robophysical modelling has shown that a realistic structural damping factor can have large impacts (up to 40% reduction) on an insect's maximum aerodynamic efficiency [28], depending on the quality factor of its resonance curve. In the present work we add the insight the thorax is no impediment to the generation of non-sinusoidal kinematics, which likely serve important aerodynamic functions.

Asymmetric upstroke and downstroke velocities are a relatively common feature of insect flight and may serve important aerodynamic roles, despite not significantly affecting thoracic mechanics [15,29,42]. Numerical modelling has demonstrated significant effects of upstroke–downstroke duration asymmetry on both thrust and lift production [43,44]. In particular, faster upstrokes tend to increase thrust, which may explain the consistent observations of faster upstrokes in forward insect flight at varying speeds [15]. Furthermore, the relative speeds of upstroke and downstroke have been linked to controlling body pitch [45]. Therefore, a structurally damped thorax may not require additional muscle force tuning while adjusting duty factor to manoeuvre its body or generate enhanced forward propulsion. Our results suggest that insect flight models that approximate wingstrokes as symmetric likely generalize quite well at the level of thoracic mechanics, although this is likely not true for aerodynamics. While the thorax material properties are frequency independent, overall inertial costs change with frequency because wing inertia and aerodynamic added mass effects scale with acceleration of the wing, i.e. frequency squared [46]. As such, our results suggest that any frequency dependence of the integrated flight system cannot come from the thorax, allowing such properties to be attributed to the wings and muscles.

4.2. Implications of a flat frequency response of the exoskeleton

Our white noise tests support the hypothesis that the thorax acts like a structurally damped material even under irregular deformations that encompass a wide band of frequencies. The invariance of thorax stiffness and damping with frequency during white noise implies that there is no frequency-dependent filtering of mechanical stimuli at least up to the natural wing beat frequency of 25 Hz, and likely higher given the properties of a structurally damped system. Since the white noise stimuli were agnostic to tension or compression, this confirms that the thorax is frequency independent regardless of when in an oscillation that non-sinusoidality occurs. This result has implications for insects like *Manduca* that transiently modify their wingbeat frequency in the air on within-wingstroke timescales or experience transient perturbations.

Downloaded from https://royalsocietypublishing.org/ on 22 May 2023

Thoracic mechanics play an important role in dictating the resonant properties of a flapping insect. Substantial frequency modulation may indicate that an insect does not beat its wings at the resonant frequency of its flight system, since operation at resonance generally implies a large energetic cost for rapid frequency changes. Such off-resonance wingbeat frequencies may incur a trade-off between perturbation robustness and energetic efficiency [28,34]. In synchronous insects like hawkmoths, a neural driving frequency determines wingbeat frequency and must be modified to facilitate wingbeat frequency changes. Therefore, significant frequency-dependent thorax mechanics may have to be accounted for by the nervous system to create a transient deviation from steady state. For example, frequency-dependent stiffening would necessitate additional muscle force to drive the system more quickly. Frequency-dependent damping would necessitate force being applied at a different phase of activation than the normal phase at steady state. For a hawkmoth, our results suggest that the same phase and magnitude of muscle force could achieve frequency modulation, which may be highly advantageous under circumstances such as takeoff and landing, where wingbeat frequency changes quickly.

Recent theoretical advances in nonlinear elasticity have demonstrated that insects with substantial series compliance in their flight systems may exhibit wide, band-type resonance [47,48]. The likely source of such series elastic effects is the wing hinge, which is also the primary dissipative component of the hawkmoth thorax [19]. In these cases, there may be a range of frequencies over which efficient flight is possible, and frequency modulation within this range would not incur the loss of efficiency as a classical resonator. Estimates of frequency modulation in free-flying hawkmoths yield approximately ±15% of normal wingbeat frequency [35]. A large degree of series compliance in a dissipative wing hinge, combined with substantial frequency modulation presents an extremely difficult control task for a strongly frequency-dependent system, since the phase lag introduced by series elasticity would change with frequency. By contrast, a structurally damped wing hinge would mitigate some of this control difficulty by maintaining a constant phase lag. While frequency response measurements of the hawkmoth wing hinge do not exist, there is evidence of the structurally damped protein resilin in the hinges of hawkmoths, dragonflies, and locusts [5,32]. Therefore, in broad categories of insects, a structurally damped exoskeleton may ease frequency-dependent energetic and control demands during frequency modulation.

In addition to frequency modulation, a frequency-independent thorax has ramifications for perturbation rejection and recovery. Insect wings collide with objects ranging from raindrops to plant stems during flight [49,50]. Such perturbations to steady-state flight must be responded to by the flight muscles to maintain stability. The mechanical transparency (a flat frequency response) we observe between the wing and thorax in hawkmoths implies that a control force applied by the muscle to the thorax in response to a perturbation will be transmitted to the wing hinge after the same phase lag and with the same scaling, regardless of the speed of force application. Thus, modulation of muscle force would act on the wings in the same way, independent of frequency, potentially simplifying the control challenge that a moth faces in matching neural control to motor output. This may be relevant for both perturbation rejection as well as other control challenges such as during turning manoeuvres or when wings become damaged [37,45,51,52]. Due to the well-documented scaling of inertial and aerodynamic forces with frequency [46], the integrated thorax–wing system is still frequency dependent. However, our results demonstrate that muscle force can bypass the thorax as a filter, directly controlling the dynamics of the wing.

The flat frequency response of the thorax also has implications for the biomechanical pressures and constraints that apply over evolutionary timescales. Even within closely related subgroups of insects, there is sometimes wide variability in wingbeat frequency, such as in the bombycoid moths, whose wingbeat frequency range spans nearly an order of magnitude from 8 to 64 Hz [53]. A structurally damped thorax may reduce the amount of concomitant neuromuscular and exoskeletal coevolution necessary to evolve different wingbeat frequencies, contributing to the lability of wingbeat frequency as a functional trait. Furthermore, the evolution of an indirect flight system has likely contributed to the diversification of higher wingbeat frequency insects [54]. An indirect flight system is the most common configuration for flight muscles in insects, with the only significant exception being the odonates [54]. Previous proposed advantages to the indirect configuration involve the ability to actuate large amplitude wing strokes with extremely small muscle strains, making use of complex three-dimensional shape changes to create additional mechanical advantage [21,55]. If the thorax introduced substantial velocity-dependent filtering and dissipation, this would present an obvious detriment to the indirect flight configuration that would require additional coevolution from the flight muscles and neural circuitry to circumvent. Thus, it is reasonable that the presence of structural damping in the exoskeleton of primitive insects may have contributed to the ubiquity of indirect flight as a preferred method of wing actuation in extant insects.

4.3. Implications of structural damping for non-flapping movement

Frequency-independent damping likely has relevance in organisms that do not utilize flapping aerial locomotion [56]. There appear to be significant dynamic regimes in which vertebrate connective tissues such as tendons are largely frequency independent. Such frequency independence has been observed at higher strain rates, while classic viscous behaviour becomes more important at lower strain rates [57,58]. The origin of this mechanical behaviour remains unclear; however, it may be related to sliding between collagen fibers or interactions between collagen and proteoglycan matrix [59]. Frequency independence, potentially from structural damping, in these materials may be critical for high-power or impulsive movements in which viscous effects would either dissipate impractically large or dangerous amounts of energy, or interfere with control of rapid motion.

Despite having some functional similarity, the muscle architecture and elastic elements present in vertebrate locomotor systems differ in a few key ways from those in insects. Many insect muscles, such as the indirect flight muscles in hawkmoths, attach directly to the exoskeleton without any coupling elastic element [54]. In vertebrates, series elastic tendons introduce velocity-dependent dynamics that can significantly affect muscle–tendon unit behaviour, decoupling muscle and muscle–tendon unit dynamics [4,60,61]. In insects, analogous structures known as apodemes exist, but are over an order of magnitude stiffer on average than tendons. That

Downloaded from https://royalsocietypublishing.org/ on 22 May 2023

vertebrate connective tissues are materially distinct from chitinous exoskeleton but exhibit functionally similar characteristics under high-frequency loading illustrates an interesting commonality; however, it remains unclear what drives the emergence of this property across disparate species.

Fast, periodic movements encompass a large diversity of organismal locomotion (such as flapping flight) but differ fundamentally from ballistic movements performed by many animals. Recent work on ballistic locomotion has sparked a renewed usage of spring–mass–damper models to predict the flow of power from actuator input to motor output through the LaMSA framework [11,62,63]. In LaMSA systems, power amplification is achieved by slowly transferring muscle contractile energy to a spring over a long time scale and releasing it extremely quickly to surpass inherent force–velocity muscle power limitations. Many of these models ignore internal damping altogether, or only consider velocity-dependent effects [11,64]. In such 'superfast' movements, consideration of different models of damping may give rise to altered dynamics, given the high velocities and lack of explicit muscular control after the initial loading of the spring. A structurally damped ballistic limb movement would likely dissipate much less energy than an equivalent viscously damped one, resulting in more energy delivered to the desired output, or unwanted internal damage. Many of these movements are generated by invertebrates that utilize bending of stiff exoskeleton as the LaMSA spring, such as the mantis shrimp raptorial appendage, and therefore may have the necessary microstructural properties that give rise to structural damping [65,66]. Our work demonstrates a need to investigate multiple internal damping models in other systems that rely on complex energy flow to produce movement.

5. Conclusion

We find the mechanical response of the hawkmoth thorax in non-sinusoidal regimes to be consistent with phenomenological and mathematical predictions from a simple structural damping model, providing evidence that structural damping is a robust property of the thorax that extends beyond symmetric periodic conditions. The frequency-independent characteristics of structural damping render the thorax insensitive to non-sinusoidality and dynamically transparent to force inputs, allowing energy to flow unfiltered between muscle and wing, despite the large elastic structure that facilitates indirect flight actuation.

Data accessibility. Raw mechanical testing data are available on the SMARTech data repository: http://hdl.handle.net/1853/70341.

Authors' contributions. E.S.W.: conceptualization, data curation, formal analysis, investigation, methodology, visualization, writing—original draft, writing—review and editing; J.L.: conceptualization, methodology, writing—original draft, writing—review and editing; N.G.: conceptualization, funding acquisition, project administration, supervision, writing—original draft, writing—review and editing; S.S.: conceptualization, funding acquisition, project administration, resources, supervision, writing—original draft, writing—review and editing.

All authors gave final approval for publication and agreed to be held accountable for the work performed therein.

Conflict of interest declaration. We declare we have no competing interests.

Funding. This work was supported by US National Science Foundation RAISE grant no. IOS-2100858 to S.S. and N.G. and 1554790 (MPS-PoLS) and a Dunn Family Professorship to S.S. as well as the US National Science Foundation Physics of Living Systems SAVI student research network (GT node grant no. 1205878).

Acknowledgements. We thank Scott Wilburn, Dr Paul Umbanhowar and Dr Dan Goldman for access to the shaker apparatus and assistance with troubleshooting.

References

1. Roberts TJ, Azizi E. 2011 Flexible mechanisms: the diverse roles of biological springs in vertebrate movement. *J. Exp. Biol.* **214**, 353–361. (doi:10.1242/jeb.038588)
2. Griffiths RI. 1991 Shortening of muscle fibres during stretch of the active cat medial gastrocnemius muscle: the role of tendon compliance. *J. Physiol.* **436**, 219–236. (doi:10.1113/jphysiol.1991.sp018547)
3. Konow N, Azizi E, Roberts TJ. 2012 Muscle power attenuation by tendon during energy dissipation. *Proc. R. Soc. B* **279**, 1108–1113. (doi:10.1098/rspb.2011.1435)
4. Robertson BD, Sawicki GS. 2015 Unconstrained muscle-tendon workloops indicate resonance tuning as a mechanism for elastic limb behavior during terrestrial locomotion. *Proc. Natl Acad. Sci. USA* **112**, E5891–E5898. (doi:10.1073/pnas.1500702112)
5. Weis-Fogh T. 1960 A rubber-like protein in insect cuticle. *J. Exp. Biol.* **37**, 889–907. (doi:10.1242/jeb.37.4.889)
6. Tytell ED, Holmes P, Cohen AH. 2011 Spikes alone do not behavior make: why neuroscience needs biomechanics. *Curr. Opin. Neurobiol.* **21**, 816–822. (doi:10.1016/j.conb.2011.05.017)
7. Chiel HJ, Ting LH, Ekeberg Hartmann MJ. 2009 The brain in its body: motor control and sensing in a biomechanical context. *J. Neurosci.* **29**, 12 807–12 814. (doi:10.1523/JNEUROSCI.3338-09.2009)
8. Cowan NJ, Fortune ES. 2007 The critical role of locomotion mechanics in decoding sensory systems. *J. Neurosci.* **27**, 1123–1128. (doi:10.1523/JNEUROSCI.4198-06.2007)
9. Zajac FE. 1989 Muscle and tendon: properties, models, scaling, and application to biomechanics and motor control. *Crit. Rev. Biomed. Eng.* **17**, 359–411.
10. Tytell ED, Carr JA, Danos N, Wagenbach C, Sullivan CM, Kiemel T, Cowan NJ, Ankarali MM. 2018 Body stiffness and damping depend sensitively on the timing of muscle activation in lampreys. *Integr. Comp. Biol.* **58**, 860–873. (doi:10.1093/icb/icy042)
11. Ilton M *et al.* 2018 The principles of cascading power limits in small, fast biological and engineered systems. *Science* **360**, eaao1082. (doi:10.1126/science.aao1082)
12. Divi S, Ma X, Ilton M, St. Pierre R, Eslami B, Patek SN, Bergbreiter S. 2020 Latch-based control of energy output in spring actuated systems. *J. R. Soc. Interface* **17**, 20200070. (doi:10.1098/rsif.2020.0070)
13. Herrera-Amaya A, Seber EK, Murphy DW, Patry WL, Knowles TS, Bubel MM, Maas AE, Byron ML. 2021 Spatiotemporal asymmetry in metachronal rowing at intermediate reynolds numbers. *Integr. Comp. Biol.* **61**, 1579–1593. (doi:10.1093/icb/icab179)
14. Cavagna GA. 2010 Symmetry and asymmetry in bouncing gaits. *Symmetry* **2**, 1270–1321. (doi:10.3390/sym2031270)
15. Ellington C. 1984 The aerodynamics of hovering insect flight. III. Kinematics. *Phil. Trans. R. Soc. B* **305**, 41–78. (doi:10.1098/rstb.1984.0051)
16. Biewener AA, Daley MA. 2007 Unsteady locomotion: integrating muscle function with whole body dynamics and neuromuscular control. *J. Exp. Biol.* **210**, 2949–2960. (doi:10.1242/jeb.005801)
17. Pringle S. 1940 The excitation and contraction of the flight muscles of insects. *J. Physiol.* **108**, 226–232. (doi:10.1113/jphysiol.1949.sp004326)
18. Dickinson MH, Lehmann FO, Chan WP. 1998 The control of mechanical power in insect flight. *Am. Zool.* **38**, 718–728. (doi:10.1093/icb/38.4.718)
19. Gau J, Gravish N, Sponberg S. 2019 Indirect actuation reduces flight power requirements in *Manduca sexta* via elastic energy exchange. *J. R. Soc. Interface* **16**, 20190543. (doi:10.1098/rsif.2019.0543)

Downloaded from https://royalsocietypublishing.org/ on 22 May 2023

20. Ando N, Kanzaki R. 2016 Flexibility and control of thorax deformation during hawkmoth flight. *Biol. Lett.* **12**, 20150733. (doi:10.1098/rsbl.2015.0733)
21. Deora T, Gundiah N, Sane SP. 2017 Mechanics of the thorax in flies. *J. Exp. Biol.* **220**, 1382–1395. (doi:10.1242/jeb.128363)
22. Jankauski MA. 2020 Measuring the frequency response of the honeybee thorax. *Bioinspiration Biomim.* **15**, 046002. (doi:10.1088/1748-3190/ab835b)
23. Weaver Jr W, Timoshenko SP, Young DH. 1991 *Vibration problems in engineering*. Chichester, UK: John Wiley & Sons.
24. Drucker DC. 2021 Coulomb friction, plasticity, and limit loads. *J. Appl. Mech.* **21**, 71–74. (doi:10.1115/1.4010821)
25. Muravskii GB. 2004 On frequency independent damping. *J. Sound Vib.* **274**, 653–668. (doi:10.1016/j.jsv.2003.05.012)
26. Gosline J, Lillie M, Carrington E, Guerette P, Ortlepp C, Savage K. 2002 Elastic proteins: biological roles and mechanical properties. *Phil. Trans. R. Soc. B* **357**, 121–132. (doi:10.1098/rstb.2001.1022)
27. Dudek DM, Full RJ. 2006 Passive mechanical properties of legs from running insects. *J. Exp. Biol.* **209**, 1502–1515. (doi:10.1242/jeb.02146)
28. Lynch J, Gau J, Sponberg S, Gravish N. 2021 Dimensional analysis of spring-wing systems reveals performance metrics for resonant flapping-wing flight. *J. R. Soc. Interface* **18**, 20200888. (doi:10.1098/rsif.2020.0888)
29. Willmott AP, Ellington CP. 1997 The mechanics of flight in the hawkmoth *Manduca sexta* I. Kinematics of hovering and forward flight. *J. Exp. Biol.* **200**, 2705–2722. (doi:10.1242/jeb.200.21.2705)
30. Zanker JM. 1990 The wing beat of *Drosophila melanogaster*. I. Kinematics. *Phil. Trans. R. Soc. Lond. B* **327**, 1–18. (doi:10.1098/rstb.1990.0040)
31. Gravish N, Franklin SV, Hu DL, Goldman DI. 2012 Entangled granular media. *Phys. Rev. Lett.* **108**, 208001. (doi:10.1103/PhysRevLett.108.208001)
32. Hollenbeck AC, Palazotto AN. 2013 Mechanical characterization of flight mechanism in the hawkmoth *Manduca sexta*. *Exp. Mech.* **53**, 1189–1199. (doi:10.1007/s11340-013-9726-5)
33. Weis-Fogh T. 1972 Energetics of hovering flight in hummingbirds and in Drosophila. *J. Exp. Biol.* **56**, 79–104. (doi:10.1242/jeb.56.1.79)
34. Gau J, Wold ES, Lynch J, Gravish N, Sponberg S. 2022 The hawkmoth wingbeat is not at resonance. *Biol. Lett.* **18**, 20220063. (doi:10.1098/rsbl.2022.0063)
35. Gau J, Gemilere R, Lds-Vip LJ, Gravish N, Sponberg S. 2021 Rapid frequency modulation in a resonant system: aerial perturbation recovery in hawkmoths. *Proc. R. Soc. B* **288**, 20210352. (doi:10.1098/rspb.2021.0352)
36. Ortega-Jimenez VM, Greeter JS, Mittal R, Hedrick TL. 2013 Hawkmoth flight stability in turbulent vortex streets. *J. Exp. Biol.* **216**, 4567–4579. (doi:10.1242/jeb.089672)
37. Fernandez MJ, Springthorpe D, Hedrick TL. 2012 Neuromuscular and biomechanical compensation for wing asymmetry in insect hovering flight. *J. Exp. Biol.* **215**, 3631–3638. (doi:10.1242/jeb.073627)
38. Fernandez MJ, Driver ME, Hedrick TL. 2017 Asymmetry costs: effects of wing damage on hovering flight performance in the hawkmoth *Manduca sexta*. *J. Exp. Biol.* **220**, 3649–3656. (doi:10.1242/jeb.153494)
39. Kihlstrom K, Aiello B, Warrant E, Sponberg S, Stockl A. 2021 Wing damage affects flight kinematics but not flower tracking performance in hummingbird hawkmoths. *J. Exp. Biol.* **224**, jeb236240. (doi:10.1242/jeb.236240)
40. Tu MS, Daniel TL. 2004 Cardiac-like behavior of an insect flight muscle. *J. Exp. Biol.* **207**, 2455–2464. (doi:10.1242/jeb.01039)
41. Tu MS, Daniel TL. 2004 Submaximal power output from the dorsolongitudinal flight muscles of the hawkmoth *Manduca sexta*. *J. Exp. Biol.* **207**, 4651–4662. (doi:10.1242/jeb.01321)
42. Weis-Fogh T, Jensen M. 1956 Biology and physics of locust flight. I. Basic principles in insect flight. A critical review. *Phil. Trans. R. Soc. B* **239**, 415–458. (doi:10.1098/rstb.1956.0007)
43. Yu Y, Tong B. 2005 Flow control mechanism in wing flapping with stroke asymmetry during insect forward flight. *Acta Mechanica Sinica/Lixue Xuebao* **21**, 218–227. (doi:10.1007/s10409-005-0032-z)
44. Younsi A, El-Hadj AA, Abd Rahim SZ, Rezoug T. 2022 Effects of the wing spacing, phase difference, and downstroke ratio on flapping tandem wings. *Proc. Inst. Mech. Eng. C: J. Mech. Eng. Sci.* **236**, 4689–4712. (doi:10.1177/09544062211045184)
45. Cheng B, Deng X, Hedrick TL. 2011 The mechanics and control of pitching manoeuvres in a freely flying hawkmoth (*Manduca sexta*). *J. Exp. Biol.* **214**, 4092–4106. (doi:10.1242/jeb.062760)
46. Sane SP. 2003 The aerodynamics of insect flight. *J. Exp. Biol.* **206**, 4191–4208. (doi:10.1242/jeb.00663)
47. Pons A, Beatus T. 2022 Distinct forms of resonant optimality within insect indirect flight motors. *J. R. Soc. Interface* **19**, 20220080. (doi:10.1098/rsif.2022.0080)
48. Pons A, Beatus T. 2022 Elastic-bound conditions for energetically optimal elasticity and their implications for biomimetic propulsion systems. *Nonlinear Dyn.* **108**, 2045–2074. (doi:10.1007/s11071-022-07325-6)
49. Dickerson AK, Shankles PG, Madhavan NM, Hu DL. 2012 Mosquitoes survive raindrop collisions by virtue of their low mass. *Proc. Natl Acad. Sci. USA* **109**, 9822–9827. (doi:10.1073/pnas.1205446109)
50. Foster DJ, Cartar RV. 2011 What causes wing wear in foraging bumble bees? *J. Exp. Biol.* **214**, 1896–1901. (doi:10.1242/jeb.051730)
51. Mountcastle AM, Alexander TM, Switzer CM, Combes SA. 2016 Wing wear reduces bumblebee flight performance in a dynamic obstacle course. *Biol. Lett.* **12**, 20160294. (doi:10.1098/rsbl.2016.0294)
52. Beatus T, Guckenheimer JM, Cohen I. 2015 Controlling roll perturbations in fruit flies. *J. R. Soc. Interface* **12**, 20150075. (doi:10.1098/rsif.2015.0075)
53. Aiello BR, Sikandar UB, Minoguchi H, Bhinderwala B, Hamilton CA, Kawahara AY, Sponberg S. 2021 The evolution of two distinct strategies of moth flight. *J. R. Soc. Interface* **18**, 20210632. (doi:10.1098/rsif.2021.0632)
54. Dudley R. 2002 *The biomechanics of insect flight: form, function, evolution*. Princeton, NJ: Princeton University Press.
55. Boettiger E, Furshpan E. 1952 The mechanics of flight movements in Diptera. *Biol. Bull.* **102**, 200–211. (doi:10.2307/1538368)
56. Ker RF. 1977 Some structural and mechanical properties of locust and beetle cuticle. PhD thesis, University of Oxford, UK.
57. Rosario MV, Roberts TJ. 2020 Loading rate has little influence on tendon fascicle mechanics. *Front. Physiol.* **11**, 255. (doi:10.3389/fphys.2020.00255)
58. Crisco JJ, Moore DC, McGovern RD. 2002 Strain-rate sensitivity of the rabbit MCL diminishes at traumatic loading rates. *J. Biomech.* **35**, 1379–1385. (doi:10.1016/S0021-9290(02)00167-7)
59. Bonner TJ, Newell N, Karunaratne A, Pullen AD, Amis AA, Bull A MJ, Masouros SD. 2015 Strain-rate sensitivity of the lateral collateral ligament of the knee. *J. Mech. Behav. Biomed. Mater.* **41**, 261–270. (doi:10.1016/j.jmbbm.2014.07.004)
60. Duenwald SE, Vanderby R, Lakes RS. 2009 Viscoelastic relaxation and recovery of tendon. *Ann. Biomed. Eng.* **37**, 1131–1140. (doi:10.1007/s10439-009-9687-0)
61. Daley MA, Biewener AA. 2011 Leg muscles that mediate stability: mechanics and control of two distal extensor muscles during obstacle negotiation in the guinea fowl. *Phil. Trans. R. Soc. B* **366**, 1580–1591. (doi:10.1098/rstb.2010.0338)
62. Longo SJ, Cox SM, Azizi E, Ilton M, Olberding JP, St Pierre R, Patek SN. 2019 Beyond power amplification: latch-mediated spring actuation is an emerging framework for the study of diverse elastic systems. *J. Exp. Biol.* **222**, jeb197889. (doi:10.1242/jeb.197889)
63. Sutton GP, Mendoza E, Azizi E, Longo SJ, Olberding JP, Ilton M, Patek SN. 2019 Why do large animals never actuate their jumps with latch-mediated springs? Because they can jump higher without them. *Integr. Comp. Biol.* **59**, 1609–1618. (doi:10.1093/icb/icz145)
64. Bolmin O, Socha JJ, Alleyne M, Dunn AC, Fezzaa K, Wissa AA. 2021 Nonlinear elasticity and damping govern ultrafast dynamics in click beetles. *Proc. Natl Acad. Sci. USA* **118**, e2014569118. (doi:10.1073/pnas.2014569118)
65. Farley GM, Wise MJ, Harrison JS, Sutton GP, Kuo C, Patek SN. 2022 Correction: Adhesive latching and legless leaping in small, worm-like insect larvae. *J. Exp. Biol.* **225**, jeb243841. (doi:10.1242/jeb.243841)
66. Patek SN, Korff WL, Caldwell RL. 2004 Deadly strike mechsanism of a mantis shrimp. *Nature* **428**, 819–820. (doi:10.1038/428819a)